Microwave Oven Mode Tuning by Slab Dielectric Loads

THEODORE G. MIHRAN, FELLOW, IEEE

Abstract—**Cold-test measurements have been made of mode tuning in a microwave oven cavity containing a slab water load of variable height. Two distinct types of mode behavior are observed: 1) a mode which is tuned generally upward in frequency, proceeding in sawtooth steps, and 2) a mode whose resonant frequency is nearly constant, except for slight downward perturbations at regular intervals.**

Two theoretical treatments are presented to understand and verify the observed mode behavior. A plane wave analysis is found to illustrate most of the qualitative aspects of mode tuning, such as its stairstep behavior and the phenomenon of mode linking by loss. A more accurate, quantitative description of mode behavior is obtained by generalizing dispersion relationships which have been developed in the past for the analysis of rectangular waveguides with dielectric slabs.

Agreement between theory and measurement is good in general, except for light loads in case 2 above.

I. Introduction

IN SPITE of the rapidly growing commercial importance of microwave ovens, their design remains primarily an empirical art. In 1976 Osepchuk [1] attributed the lack of oven theory to "the over-whelming complexity of the oven-food configuration as an object for study involving Maxwell's equations." This paraphrases the observation made ten years earlier by Püschner [2] that the presence of a dielectric load in a microwave oven creates a situation in which "cavity resonance is very involved and can only be clarified in the end by experiment."

Recently a computer program for the general analysis of simple dielectric discontinuities in three-dimensional structures has been developed [3]. This program appears to be well suited for numerical studies of microwave oven mode tuning by dielectric loads. To use such a program effectively it is useful to study first the related one- and two-dimensional cases as is done here. These studies provide general insights into the true nature of the three-dimensional problem and can guide the application of the more accurate (but more expensive) model to only those cases which are most significant.

A one-dimensional analysis of the effect of a slab of lossy dielectric on the resonant frequency of the space bounded by two metallic planes is given in Section II. This analysis discloses a number of concepts that are fundamental to mode tuning in microwave ovens. A problem more closely related to the geometry of practical microwave ovens can be solved rather easily, namely that of a rectangular cavity containing a lossy dielectric slab which completely fills two of the three cavity dimensions. The analysis of this case, presented in Section IV, shows that mode tuning for a given dielectric fill ratio is greatly reduced compared to the one-dimensional case of Section II.

In order to verify the validity of the analysis given in Section IV, a detailed set of mode tuning measurements was made in a commercial 915-MHz microwave oven which had been modified to accept a slab water load. These cold-test measurements, presented in Section III, indicate that two resonant modes dominate the transmission characteristic of this oven over the frequency range from 900 to 1100 MHz. One of these modes is adequately described by the theory presented in Section IV. Some aspects of the tuning of the other mode are described reasonably well by the present theory, but for light loads it is evident that the analysis given here needs further modification.

II. Parallel Plane TEM-Mode Analysis

A. Lossless Dielectric

Consider two parallel metallic planes at $z=0$ and $z=h$, as indicated by the upper and lower lines in Fig. 1(a). For TEM wave propagation in the z direction this structure will resonate at frequencies for which the plate spacing h is an integral number of half wavelengths. In MKS units the resonant frequencies are

$$f_{on}=3\times 10^8\, n/2h, \qquad n=1,2,3\cdots. \tag{1}$$

Between the plates in Fig. 1(a) consider that a dielectric sheet extends from $z=0$ to $z=d$, defining region 2. The volume above the sheet is defined as region 1. If the relative dielectric constant ϵ of the sheet is greater than unity, additional electric field energy will be stored in the sheet and all of the resonant frequencies given by (1) will be reduced. The equation which establishes resonant frequency as a function of the fraction d/h of the space occupied by the dielectric sheet can be written by inspection, referring to the equivalent transmission line circuit shown in Fig. 1(b). By taking a reference plane at the surface of the dielectric and noting that the impedance $Z_{01}\tan k_1(h-d)$ looking in the $+z$ direction must equal the negative of the impedance seen in the $-z$ direction one obtains the expression

Manuscript received April 19, 1977; revised July 22, 1977.

The author is with the Signal Processing and Communication Laboratory, Corporate Research and Development, General Electric Company, Schenectady, NY 12345.

0018-9480/78/0600-0381$00.75

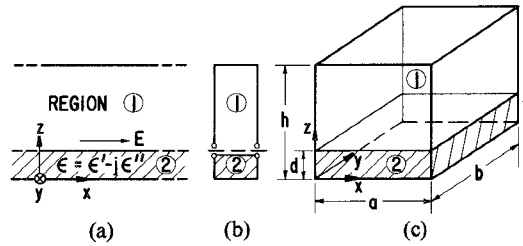

Fig. 1. (a) Configuration for plane wave analysis. (b) Equivalent circuit at dielectric surface. (c) Resonant cavity with dielectric slab at bottom, completely filling x and y dimensions.

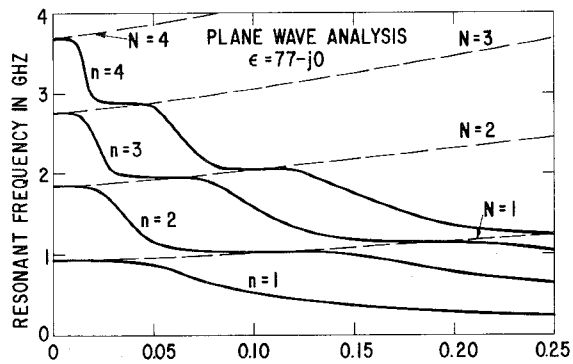

Fig. 2. Tuning of the first four modes by a lossless dielectric slab with $\epsilon = 77 - j0$. Plane wave analysis, $h = 6.4176''$.

$$Z_{01} \tan k_1(h-d) = -Z_{02} \tan k_2 d \qquad (2)$$

where $Z_{01} = 377$, $Z_{02} = 377/\sqrt{\epsilon}$, $k_1 = 2\pi f_{on}/3 \times 10^8$, and $k_2 = k_1\sqrt{\epsilon}$. Since (2) is a transcendental equation for f_{on} as a function of d/h, solutions must be obtained by numerical means.

A typical set of solutions of (2), calculated for $\epsilon = 77 + j0$ and $h = 6.4176''$, is shown in Fig. 2. In this plot, the resonant frequencies of the four lowest modes ($n = 1$ to 4) are shown as a function of the fill ratio d/h. For $d/h = 0$ the resonant frequencies are integrally spaced, i.e., $f_{on} =$ 920, 1840, 2760, and 3680 MHz. Note that the plate spacing for this example has been chosen to make the lowest order mode occur in the 915-MHz ISM band for zero fill ratio.

As the dielectric thickness is increased, Fig. 2 shows that all resonant frequencies decrease as anticipated, but the frequencies fall in stairstep fashion rather than smoothly. This behavior occurs because when there is a voltage minimum in the vicinity of the dielectric surface, the change in stored energy with d/h is minimized, therefore, the resonant frequency versus d/h curves exhibit a plateau. This occurs near $d/h = 0$ and also when the dielectric sheet is approximately an integral number of half-wavelengths thick measured in the dielectric. On the other hand when the dielectric sheet is an odd number of quarter wavelengths thick, there is a voltage maximum at the dielectric surface, and the rate of change of stored energy with d/h is maximized. At these points in Fig. 2 the resonant frequencies drop rapidly.

Another notable feature of Fig. 2 is that the plateaus of the curves cluster about slowly upward-rising curves, indicated by the dashed lines. These lines can readily be shown to be solutions of the case in region 1, for which the dielectric surface at $z = d$ is replaced by a metallic conductor. In this case (1) may be used to calculate the resonant frequencies explicitly except that the plate spacing is now $h - d$, thus

$$f_{oN} = 1.5 \times 10^8 \, N/(h-d), \qquad N = 1,2,3 \cdots. \qquad (3)$$

The dashed line curves in Fig. 2 are the solutions of (3) for $N = 1$ to 4. Note that two mode numbering systems are used in Fig. 2. The lower case letter n refers to the *total* number of standing wave maxima in the air and the dielectric combined, whereas the upper case letter N refers to the number of voltage maxima *in the air* over the dielectric. In the case of lossy dielectrics it will become evident that the latter mode numbering system is preferred.

For a different dielectric constant the location of a given plateau in Fig. 2 will shift to a different d/h. However, regardless of dielectric constant, all curves will cluster about the same rising lines shown in Fig. 2. This behavior occurs because when the dielectric sheet is an integral number of half wavelengths thick, the metal plate at $z = 0$ is effectively transformed to the dielectric surface, regardless of the dielectric constant.

B. Lossy Dielectric

The effect of loss in the dielectric may be included in the above analysis [4] by replacing ϵ by $\epsilon' - j\epsilon''$. In this case the right-hand side of (2) becomes complex. The resonant condition is specified by equating the *real* parts of the two sides of (2):

$$Z_{01} \tan k_1(h-d) = -\mathrm{Re}\left[Z_{02} \tan k_2 d\right]. \qquad (4)$$

The left-hand side of (4) remains pure real because it is not a function of ϵ. The imaginary part of (2) indicates that there must be a flow of power into the dielectric to supply its losses. Actually, this power must be supplied at the $z = h$ plane, hence the assumption of a metal plane at this point constitutes an approximation. In practice, a metallic plane is used at this point and a coupling probe or loop is used to transfer power through this plane. For reasonably high Q's (4) is an acceptable definition of resonance, although it should be recognized that this may not always be the case in a practical microwave oven.

The presence of loss has a very significant effect on the curves of Fig. 2. Over the frequency range from 900 to 4000 MHz the loss tangent ϵ''/ϵ' of tap water [5] varies from 0.05 to 0.21; ϵ' remains relatively constant at 77. For strict accuracy the variation of ϵ'' with frequency should be included in the calculations. However, since the goal in this section is primarily qualitative rather than quantitative, mode tuning curves have been calculated for an assumed constant loss tangent of 0.13 ($\epsilon = 77 - j10$) independent of frequency. When this is done the mode tuning curves shown in Fig. 3 are obtained.

It is evident from Fig. 3 that the n modes which were distinct in Fig. 2 are now merged and form a continuous set of N modes which are centered about the rising N-mode lines. This is the reason for the earlier statement

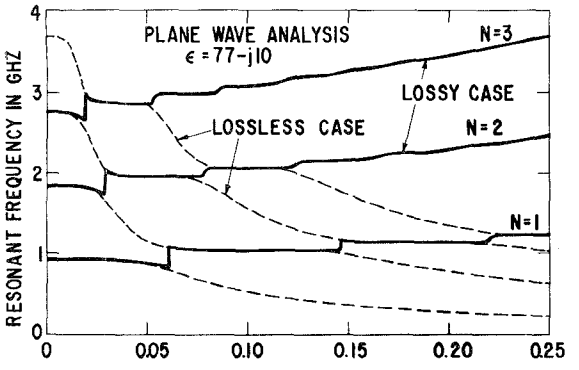

Fig. 3. Tuning of the first four modes by a lossy dielectric slab with $\epsilon = 77 - j10$. Plane wave analysis, $h = 6.4176''$.

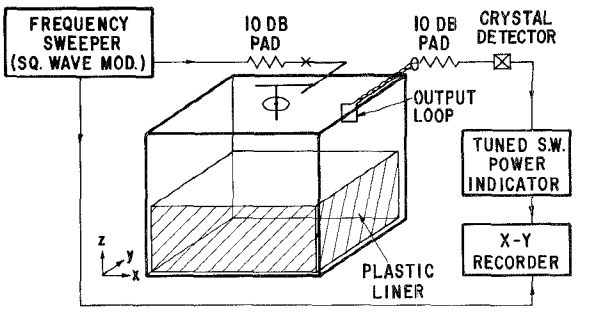

Fig. 4. Diagram of setup for measuring mode tuning in a GE Model J845003 microwave oven cavity.

that when loss is present, it is better to characterize the resonant modes by the number of voltage maxima *above* the dielectric rather than by the total number of maxima in the air and dielectric combined. Comparing Fig. 3 with Fig. 2, note that for a given dielectric thickness the presence of loss in general reduces the number of modes available for interaction in a given frequency range.

The effect of varying ϵ'' is found to be minimal. It is noticeable only at the rapidly rising portions of the curves in Fig. 3 where it is found to affect the degree of rounding only slightly.

The behavior of mode tuning with dielectric thickness in the parallel-plane case can be summarized as follows:

1) In the lossless case the resonant frequencies of all modes decrease, although the plateaus of the various modes cluster about upward-rising lines.

2) In the lossy case modes are linked together and it is more meaningful to identify resonances in terms of the number of voltage maxima outside the dielectric. In this case the general trend of resonant frequency is upward, although it occurs in a stairstep fashion.

3) In the limit of high conductivity all modes are detuned upward smoothly and these modes constitute the curves about which the solutions for the other two cases cluster.

The same qualitative features can be seen from the results of the rectangular cavity analysis presented in Section IV. However, it will be shown that the magnitude of mode tuning is reduced significantly in the rectangular cavity.

III. Measurement of Mode Tuning in a Microwave Oven

The initial objective of the work on microwave ovens presented here was to make a set of mode tuning measurements which could be compared *quantitatively* with a set of mode tuning calculations. Cold test mode measurements were made on a GE Model J845003 free-standing range, which was designed to operate in the 915-MHz ISM band.

To reduce the complexity of the mode structure in the oven of this unit, the following changes were made (see Fig. 4).

1) The mode stirrer, the metal rack, the bake and broil heating elements, the thermostat, and other small projections into the oven were removed.

2) The oven was turned upside down so that the input antenna was at the top rather than at the bottom.

3) A plastic liner was form fitted to the lower half of the oven so that the entire cross section of the oven could be occupied by a water load.

4) The capacitive loading disc was removed from the end of the input antenna so that the Q's of all resonances would be high enough to be observed individually.

5) A small output loop, approximately one square inch in area, was located in the x-z plane at the middle of the edge formed by the top and right side of the overturned oven.

For cold test purposes the magnetron was removed as the power source and replaced with a Hewlett–Packard Model 691D square-wave modulated frequency sweeper. Approximately 1 ft of RF coaxial line, containing several bends, was left in place between the sweeper line and the input antenna, as indicated by the heavy lines in Fig. 4. Attenuator pads were placed in the input and output lines just outside the oven to reduce spurious resonances not associated with the oven itself. The ouput signal was detected by a crystal and a HP Model 415B standing-wave indicator. The output of the indicator was recorded on an x-y recorder over frequency range from 900 to 1100 MHz. The sweeper calibration was found to be accurate to ± 5 MHz.

With the placement of the input antenna and output loop as described above, a fairly clean two-peak transmission characteristic was observed for most load conditions. A typical set of transmission patterns is shown in Fig. 5 for water volumes ranging from 5.25 to 9.0 l in 0.25-l steps. Clearly evident in this figure are the two modes. The upper mode holds fairly constant in frequency at 1050 MHz. The lower frequency mode initially drifts down in frequency, disappears, then reappears at a higher frequency only to drift downward again.

The total volume of the oven was 104 l. Patterns similar to those shown in Fig. 5 were recorded as the water volume was increased from zero to 25 l in 0.25-l steps. A typical set of patterns for heavy loading (17.25–21 l) is shown in Fig. 6. The splitting of the lower peak in Fig. 6

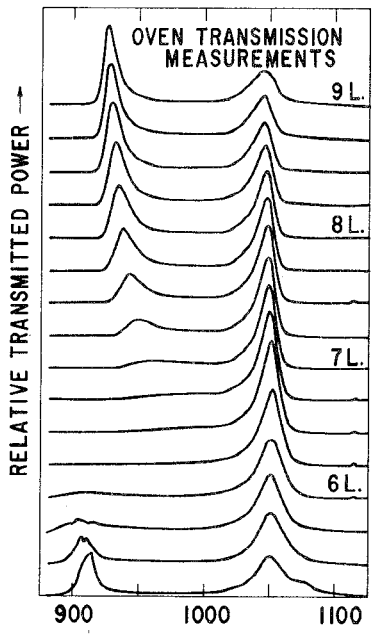

Fig. 5. Measured power transmission versus frequency in modified GE oven for water volumes between 5.25 and 9 l.

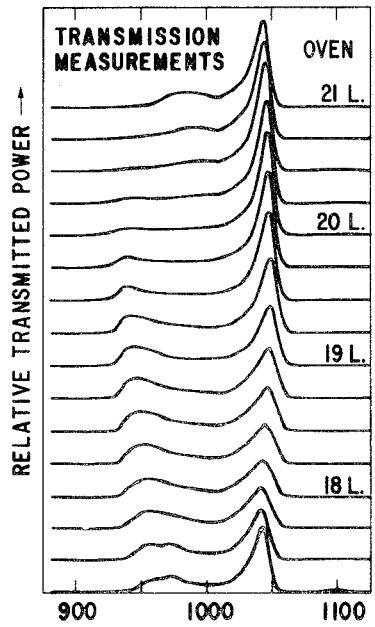

Fig. 6. Measured power transmission versus frequency in modified GE oven for water volumes between 17.25 and 21 l.

will be discussed in Section IV. From recording the resonant frequencies indicated on one hundred transmission patterns like those shown in Fig. 5 and Fig. 6 the mode tuning plots shown in Fig. 7(a) were made.

The two dominant modes shown in Fig. 7(a) behave in distinctly different manners. The lower frequency mode, the so-called "cooking" mode, starts at 915 MHz and initially is tuned downward. As the water level is increased, however, it fades out of sight only to reappear at a higher frequency than it initially was. Subsequently, this mode sawtooths its way upward in frequency in a manner reminiscent of the modes shown in Fig. 3, although in Fig. 7(a) the plateaus are tilted rather than horizontal.

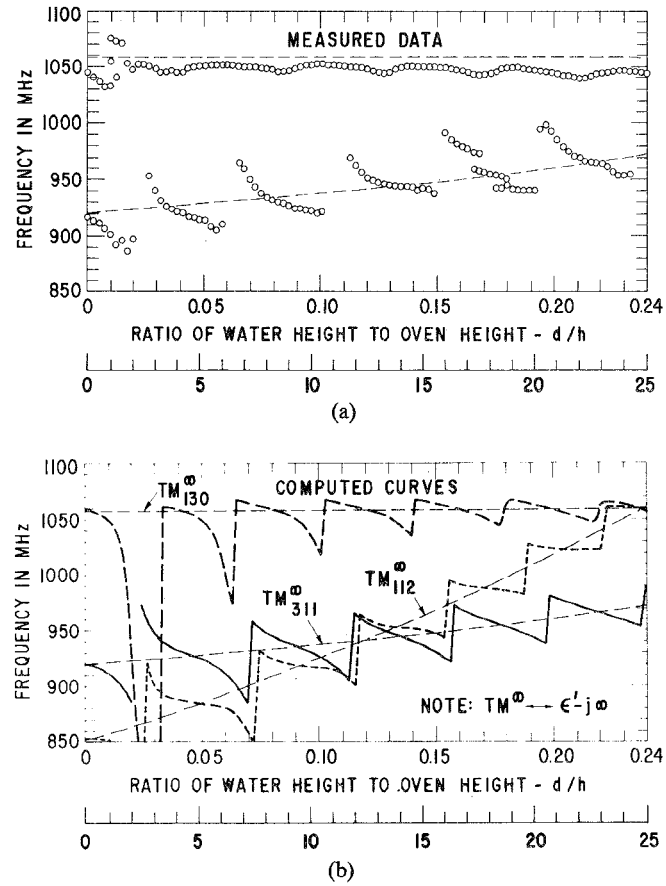

Fig. 7. (a) Measured mode tuning versus water volume for two modes in modified GE oven. (b) Computed mode tuning versus water volume for TM_{130} mode (long dashes), TM_{311} mode (solid), and TM_{112} mode (short dashes).

On the other hand, the mode at 1050 MHz is seen from Fig. 7(a) to change in frequency only slightly. This behavior is depicted very clearly in Fig. 5 and Fig. 6. Careful examination of these patterns discloses slight periodic downward excursions, however, as indicated in Fig. 7(a).

Note that the lower mode in Fig. 7(a) is tuned upward in frequency by about 50 MHz for the case of $d/h = 0.24$. Over this frequency range the data exhibit five upward steps. The results of the plane wave analysis shown in Fig. 3 exhibit the same qualitative behavior—upward tuning in stepwise fashion—but the steps are fewer in number and the tuning for $d/h = 0.24$ is six times greater in Fig. 3 than in Fig. 7(a). In the next section the plane wave analysis is modified to apply to three-dimensional resonant cavities with slab loads.

IV. Analysis of a Resonant Cavity with a Dielectric Slab

Theory: The development in this section follows the treatment by Marcuvitz for propagation in rectangular wavelengths containing dielectric slabs [6]. His analysis is limited to a full-width slab which is placed either along the bottom or along the sidewall of the guide. The analysis given below extends the results of Marcuvitz, developed for the dominant mode in waveguides, to resonant rectangular cavities containing higher order modes.

Referring to Fig. 1(c) Marcuvitz treats the waveguide that would be formed by extending this geometry in the y direction. He obtains an expression for the guide wavelength $\lambda_{g(y)}$ in the y direction. This expression is also useful for cavity analysis since metallic walls may be placed at planes separated by an integral number of half-guide wavelengths in the y direction, i.e.,

$$b = m\lambda_{g(y)}/2, \qquad m = 1,2,3\cdots. \tag{5}$$

Although Marcuvitz is concerned with propagation in the y direction, he utilizes the "transverse resonance" method for obtaining the propagation characteristics. In this method one considers the composite guide at the cutoff frequency for propagation in the y direction. At this frequency propagation is solely in the transverse direction which is normal to the dielectric surface, i.e., the z direction in Fig. 1(c). Two cases can be differentiated: 1) the TE mode in which the E lines lie in the plane of the dielectric surface, and 2) the TM mode in which the E lines are normal to the plane of the dielectric. Note that in the latter case the H lines lie in the plane of the dielectric surface. The TE mode configuration is similar to the one-dimensional case analyzed in Section II. The TM mode case has no obvious plane wave resonance counterpart.

The equivalent transmission line circuit of Fig. 1(b) can still be used for either the TE or TM case provided Z_0 is defined appropriately for the dielectric constant of the transmission line and the type of mode, namely,

$$Z_{TE} = (377/\sqrt{\epsilon})(\lambda_g/\lambda_\infty) \tag{6}$$

$$Z_{TM} = (377/\sqrt{\epsilon})(\lambda_\infty/\lambda_g) \tag{7}$$

where $\lambda_\infty/\lambda_g = \sqrt{1-(f_c/f)^2}$, $\lambda_\infty = \lambda_0/\sqrt{\epsilon}$, $\lambda_0 = 3\times 10^8/f$, and $\lambda_g = 2\pi/k_z$. Note carefully that the guide wavelengths referred to in (6) and (7) are measured in the z direction.

Maxwell's equations lead to the wave equation

$$\nabla^2 E + k^2 E = 0 \tag{8}$$

where $k^2 = \omega^2\epsilon/(3\times 10^8)^2$. When (8) is solved in rectangular coordinates the familiar product type solution is obtained with sinusoidal field variation in the three directions characterized by propagation constants k_x, k_y, and k_z. For any component of E, (8) yields the equation

$$k_x^2 + k_y^2 + k_z^2 = k^2 = \omega^2\epsilon/(3\times 10^8)^2. \tag{9}$$

The propagation constants in the x and y directions are the same in both transmission lines in Fig. 1(b) and are set by the boundary conditions, namely,

$$k_x = \pi l/a, \qquad l = 1,2,3\cdots$$
$$k_y = \pi m/b, \qquad m = 1,2,3\cdots. \tag{10}$$

The propagation constants in the z direction are different in the two lines and are given from (9) and (10) as

$$k_{z1}^2 = (2\pi/\lambda_0)^2 - (\pi l/a)^2 - (\pi m/b)^2 \tag{11}$$

$$k_{z2}^2 = \epsilon(2\pi/\lambda_0)^2 - (\pi l/a)^2 - (\pi m/b)^2. \tag{12}$$

The guide wavelengths in the two lines are obtained from the definition of propagation constant and guide wavelength

$$k_{z1,2} = 2\pi/\lambda_{g1,2} \tag{13}$$

which in turn are related by (6) and (7) to the ratio of the characteristic impedances of the two lines

$$(Z_{01}/Z_{02})_{TE} = \epsilon(Z_{02}/Z_{01})_{TM} = k_{z2}/k_{z1}. \tag{14}$$

Inserting the ratio k_{z2}/k_{z1} from (11) and (12)

$$(Z_{01}/Z_{02})_{TE} = \epsilon(Z_{02}/Z_{01})_{TM} = \left[\frac{\epsilon(2/\lambda_{on})^2 - (l/a)^2 - (m/b)^2}{(2/\lambda_{on})^2 - (l/a)^2 - (m/b)^2}\right]^{1/2}. \tag{15}$$

Thus (4) and (15) constitute the general condition for the n resonant frequencies $f_{on} = 3\times 10^8/\lambda_{on}$ of a rectangular cavity loaded between $z=0$ and $z=d$ with a lossy dielectric slab.

The Z_0 ratios (8.1.2) and (8.2.2) of Marcuvitz [6] may be obtained from (15) by noting from (5) that the guide wavelength measured in the y direction in Fig. 1 will be $2b/m$ for a cavity. Furthermore, note that $l=1$ and $m=1$ for the dominant TM mode, and that $l=0$ and $m=1$ for the dominant TE mode, the only cases considered by Marcuvitz.

An unpublished analysis by Ataras [7] gives a result identical with (4) and (15) provided the TM definition of Z_0 is used in (15). Ataras does not obtain the TE solution because he assumed all three components of electric field E_x, E_y, and E_z are nonzero. Actually, in the TE case the E_z component must be zero. Thus this case is not included in the Ataras analysis because it would involve division by zero in his derivation.

Calculations: The dimensions of the Model J845003 oven are $a=23$ in, $b=17.25$ in, and $h=16$ in. In the empty oven $k_{z1} = \pi n/h$ and the resonant frequencies without dielectric loading may be calculated directly from (9). There are eleven TM modes in the frequency range from 850 to 1060 MHz in the empty oven. There are an equal number of TE modes at the same frequencies. These modes are listed in Table I.

Modes with the even x and y mode numbers l and m will not be excited because the input antenna is vertical

TABLE I
RESONANT TE AND TM MODES IN EMPTY OVEN, 23×17.25×16 INCHES

Mode Numbers			Resonant Frequency
L	M	n	f_0 (MHz)
1	1	2 ***	853 ***
3	0	1 ***	854 ***
2	2	0	859
2	0	2	899
3	1	1 ***	920 ***
2	2	1	932
2	1	2	962
0	2	2	1007
3	2	0	1031
1	2	2	1039
1	3	0 ***	1059 ***

***indicates modes excited by center feed voltage probe.

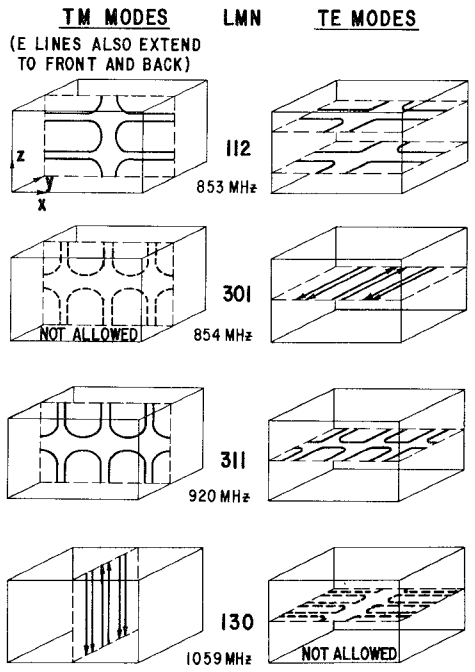

Fig. 8. Electric field patterns of selected TE and TM modes between 850 and 1060 MHz in empty oven.

and is located at the midpoints of the x and y dimensions of the oven. This leaves only four pairs of TE and TM modes to be considered, as indicated by the lines marked with asterisks in Table I. These modes are sketched in Fig. 8. It is evident that none of the TE modes in Fig. 8 will be excited because they have no E component in the direction of the exciting E field of the vertical input antenna. The TM_{301} mode cannot exist [8] because zero E-field variation in the y direction requires the E-field pattern shown by the dotted line to exist at the front and back planes, an impossible condition at metallic surfaces. Thus only three modes, all TM, remain to be considered: 112, 311, and 130. Note that the placement of the output loop is appropriate to couple at the magnetic field maximum for each of these modes.

Calculations for TM_{112}, TM_{311}, and TM_{130} mode tuning have been carried out using (4) and the TM definition of Z_0 given in (15). The computed results are shown in Fig. 7(b). The measured data in Fig. 7(a) can be compared directly with the computed curves in Fig. 7(b). The agreement for the TM_{311} mode is very good, both in overall upward tuning and in the structure. The agreement for the TM_{130} mode is quite good for large loads but for small loads the theory gives larger downward deviations than are observed. The TM_{112} mode is barely visible in the measured data, evidently because its Q is much lower than for the other two modes. Only when the Q of the TM_{311} mode is low, as in the lower patterns of Fig. 6, is the TM_{112} mode visible as it passes through the TM_{311} mode.

As an independent verification that the TE_{311} mode was not being excited, its tuning characteristic was computed using (4) and the TE definition from (15). The tuning pattern for this mode is shown in Fig. 9 as a dashed line curve. For comparison the TM_{311} tuning pattern from Fig. 7(b) is shown by the solid-line curve. The dominant characteristic of the TE mode is that the frequency remains nearly constant as it passes through the upward rising $N=1$ curve. Contrasted to this behavior the TM mode passes through the same points with a distinctly downward slope. The measured data in Fig. 7(a) display a downward slope in going through the same points, indicating that power is being transmitted through the cavity via the TM mode. Also, note from Fig. 8 that the TE_{130} mode cannot exist with zero variation in the z direction, so its possible excitation cannot be used to explain the observed constant frequency characteristic of the higher frequency mode.

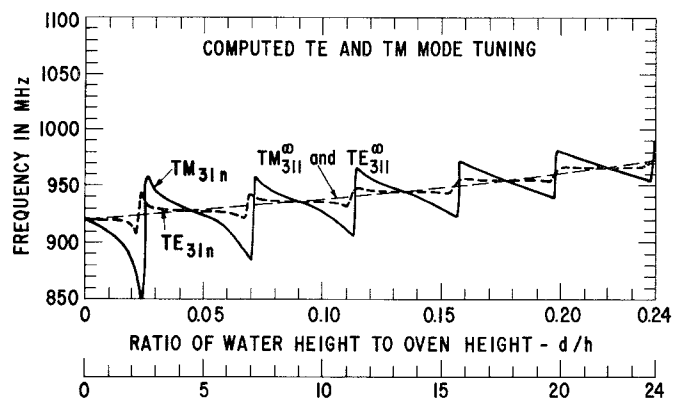

Fig. 9. Computed TE_{311} mode tuning (dash) and computed TM_{311} mode tuning (solid).

V. Conclusions

The mode tuning characteristic of a microwave oven has been measured and computed as a function of load height under idealized conditions. In the frequency range from 850 to 1060 MHz the power transmission pattern is dominated by the two modes TM_{311} and TM_{130}, both propagating in the z direction. The behavior of these modes has been computed using the transverse resonance method of Marcuvitz.

Agreement between measured and computed mode tuning behavior is satisfactory for the TM_{311} mode. For large loads agreement is good for the TM_{130} mode; for small loads the measured frequency excursions are considerably smaller than calculated, indicating that a more accurate theoretical treatment is needed.

The goal of this work was to establish a simple geometric configuration in which measurements and computations of mode tuning by dielectric loads in microwave ovens could be compared quantitatively. This goal was reached with reasonable success. A challenging goal for the future is to restore to the study as many features of a practical oven as possible—arbitrary food size and placement, heavy coupling, mode stirring, etc., and still retain the ability to made accurate and useful computations of mode tuning.

Acknowledgment

The author gratefully acknowledges informative discussions with L. H. Fitzmayer, J. E. Staats, and R. V. Prucha of the Range Department and with R. A. Dehn of CRD.

REFERENCES

[1] J. M. Osepchuk, "Microwave engineering problems in the microwave oven," presented at 1976 IEEE MTT-S Int. Microwave Symp. Cherry Hill, NJ, June 14–16, 1976.

[2] H. Püschner, *Heating With Microwaves*. New York: Springer-Verlag, 1966, p. 176.

[3] S. Akhtarzad and P. B. Johns, "Analysis of a wide range of microwave resonators: T.L.M. methods," *Electron. Lett.* vol. 11, pp. 599–606, Nov. 27, 1975.

[4] N. Marcuvitz, *Waveguide Handbook*. New York: McGraw-Hill, 1951, p. 17.

[5] A. R. Von Hippel, *Dielectric Materials and Applications*. New York: Wiley, 1954, p. 361.

[6] N. Marcuvitz, *Waveguide Handbook*. New York: McGraw-Hill, 1951, pp. 388–393.

[7] W. S. Ataras, "The field solution for a partially filled cavity," unpublished.

[8] S. Ramo and J. R. Whinnery, *Fields and Waves in Modern Radio*. New York: Wiley, 1944, p. 395.

Characteristics of Single and Coupled Microstrips on Anisotropic Substrates

NICOLAOS G. ALEXOPOULOS, MEMBER, IEEE, AND CLIFFORD M. KROWNE, MEMBER, IEEE

Abstract—**In this paper, the effect of an anisotropic substrate on the characteristics of covered microstrip is presented for single and coupled lines. The Green's function is obtained in integral and series form for an arbitrary anisotropic substrate. Computer programs based on the method of moments approach [1], [2] are employed and results are presented in graphical form for impedance Z, coupling constant K, and phase velocity v_p as functions of n_x/n_y (the ratio of the substrate indices of refraction). Z, K, and v_p are studied for various w/H, S/H, and B/H ratios where w is the line width (w_1 and w_2 for coupled lines), S is the separation between coupled lines, B is the separation between ground planes, and H is the substrate thickness.**

I. INTRODUCTION

EXTENSIVE results exist in the literature on the problem of microstrip lines on isotropic substrates, e.g., [1]–[13]. Therein, the Green's function of the problem is obtained either by image theory [7] or by a direct solution to the boundary value problem [13]. In most cases a quasi-static approach is presented, which necessitates solution to Laplace's equation for a given set of boundary conditions. A series of papers [8]–[12] presents solutions to the dispersion problem, again for isotropic substrates.

Recently [14], [15], the problem of anisotropic substrates was approached strictly from the numerical point of view. Specifically, the authors employed the method of finite differences to obtain the impedance characteristics of a single microstrip line over a single-crystal sapphire substrate. Since this crystal is uniaxial, the permittivity dyadic is strictly diagonal with a relative permittivity along the optical axis $\epsilon_y = 11.60$, while on the plane perpendicular to this axis $\epsilon_x = \epsilon_z = 9.40$. The authors proceeded to compute an equivalent isotropic relative permittivity ϵ_{req} which enables them to proceed with the computations of the microstrip characteristics.

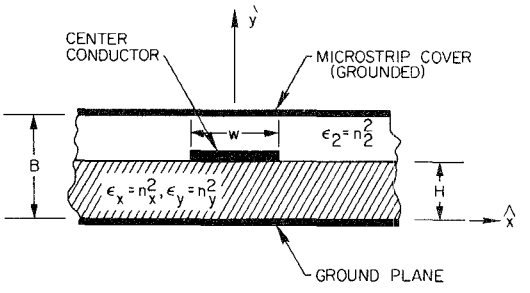

Fig. 1. Cross section of covered single microstrip geometry.

In the present paper, the problem of the anisotropic substrate is approached from the boundary value point of view. The boundary value approach necessitates the introduction of a grounded cover, although this by no means limits the usefulness of the solution since B (see Fig. 1) can be allowed to recede to infinity. An image theory approach would be much more preferable, but there appears to be no prior references on how conductors image over anisotropic media. By employing a quasi-static approach, the Green's function is incorporated into two methods of moments computer programs. These programs provide solutions to the single and coupled microstrip problem by employing the usual methods for the computation of self and mutual capacitances, characteristic impedances, and phase velocities. The results are presented for various values of the relative permittivities in the x, y, and z directions, and they are shown in Figs. 2–4 and 6 and 7.

Manuscript received August 30, 1976; revised July 15, 1977. This work was supported jointly by the U.S. Office of Naval Research under Contract N00014-76C-0896 and by the Watkins–Johnson Company.

N. G. Alexopoulos is with the Department of Electrical Sciences and Engineering, University of California, Los Angeles, CA 90024.

C. M. Krowne is with the Watkins–Johnson Company, Palo Alto, CA 94304.

0018-9480/78/0600-0387$00.75